ELSEVIER

Journal of Power Sources 68 (1997) 82–86

JOURNAL OF POWER SOURCES

Future prospects of the lithium metal anode

Zen-ichiro Takehara

Department of Chemical Engineering, Faculty of Engineering, Kansai University, Suita, Osaka 564, Japan

Accepted 9 September 1996

Abstract

Though rechargeable lithium batteries with a lithium metal anode have a high energy density compared with lithium-ion batteries with a carbon insertion anode, the poor rechargeability of the lithium anode prevents the practical use of such batteries. In this paper, several approaches studied in the author's former laboratory at Kyoto University, have been reviewed in order to improve such poor rechargeability. Poor rechargeability is caused by the formation of lithium dendrites during the charge process. The dense and thin bilayer film of LiF and Li_2O formed on the deposited lithium by the addition of the small amounts of HF and H_2O in the electrolyte may be effective for the suppression of the dendritic formation of lithium. © 1997 Published by Elsevier Science S.A.

Keywords: Rechargeable lithium batteries; Lithium metal anodes; Lithium dendrites

1. Introduction

Much effort has been expended to produce lithium secondary batteries with lithium metal anodes because of their high energy density compared with lithium-ion batteries with carbon-type insertion anodes. However, the poor rechargeability of the lithium anode prevents the practical use of such batteries. This is caused by the formation of lithium dendrites during the charging process. Such dendritic lithium either loses its electrochemical activity or grows through the separator to touch the cathode material, leading to internal short circuits. Though several approaches are currently being studied to suppress the dendritic formation of lithium during the charging process, fruitful results have not yet been obtained [1,2].

The formation of dendritic lithium is related to the interface state and reactivity between lithium and the electrolyte. Thus, it is most important to control the passivating layer on lithium by selecting a less reactive liquid electrolyte (e.g. Li_2CO_3, LiF) [3]. The formation of such passivating layers is promoted by adding agents such as CO_2 [4–7] or HF [8,9]. SnI_2 and AlI_3 are also proposed as additives to improve the lithium rechargeability [10]. Another approach to change the lithium deposition morphology has been studied by pressurizing the cell stack. Lithium is deposited densely and uniformly at the anode surface under pressure and the isolation of deposited lithium from the anode substrate during stripping is decreased [11]. Such a change of lithium deposition requires the use of polymer electrolytes [1]. These materials which, due to their solid-like nature and plasticity, are expected to be less reactive than their liquid counter parts and to be able to accommodate interfacial expansions and contractions upon cycling. A highly rechargeable lithium metal anode is expected through such extensive research in the future.

In this paper, research to suppress the dendritic formation of lithium during the charging process is reviewed.

2. Surface films on lithium and morphologies of electrodeposited lithium

The surface films on lithium immersed in various electrolytes were analyzed by X-ray photoelectron spectroscopy (XPS), Fourier-transform infrared spectroscopy (FT-IR), and scanning electron micrograph (SEM) [12–16]. The possible model for the native film formed on the lithium surface analyzed by XPS spectra is illustrated schematically in Fig. 1(a). The outer part of the native film consists of LiOH and Li_2CO_3 and the inner part consists of Li_2O. The morphologies of lithium electrodeposited on lithium metal and the surface states of lithium immersed in propylene carbonate (PC), γ-butyrolactone (γ-BL) or tetrahydrofuran (THF) containing $LiClO_4$, $LiAsF_6$, $LiBF_4$, $LiCF_3SO_3$ or $LiPF_6$ were examined. The models for the surface state of lithium immersed in PC or γ-BL containing 1.0 M $LiBF_4$ or $LiPF_6$ for 10 min or 3 days, analyzed by XPS spectra, are illustrated in Fig. 1(b)–(d). LiF in the film may be formed by the decomposition of salts, the reaction of lithium compounds

PII S0378-7753(96)02546-3

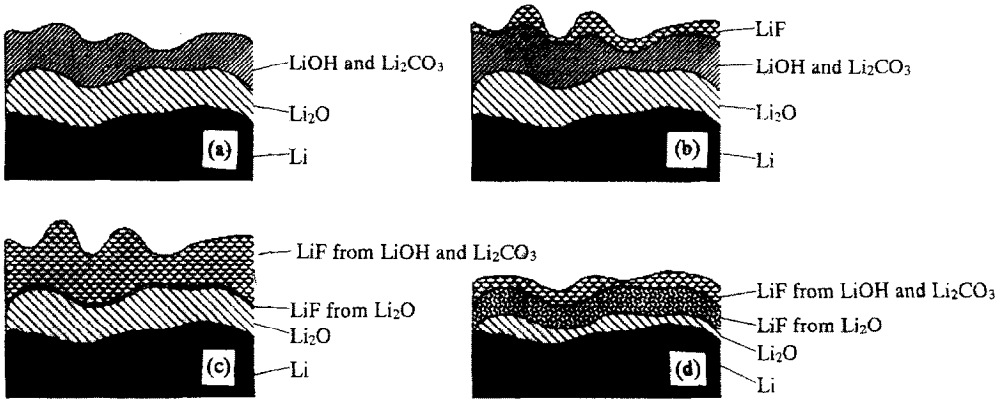

Fig. 1. Schematic illustration of: (a) as-received lithium surface; (b) lithium surface immersed in PC or γ-BL containing 1.0 M $LiBF_4$ or $LiPF_6$ for 10 min; (c) in PC or γ-BL containing 1.0 M $LiBF_4$ for 3 days, and (d) in PC or γ-BL containing 1.0 M $LiPF_6$ for 3 days.

occurring in the native film with HF existing in electrolyte as an impurity, or by the decomposition of salts in electrolyte. The surface film on lithium immersed in PC or γ-BL containing $LiPF_6$ for 3 days consists of the dense LiF and underlying thin Li_2O layer, as shown in Fig. 1(d). The surface films on lithium immersed in THF electrolyte were different from those immersed in PC and γ-BL electrolyte. XPS spectra for the lithium surface immersed in THF containing various salts showed a large amount of C, in addition to F. This indicates that a large amount of organic compounds, e.g. lithium alkoxides are formed in the LiF layer. This is caused by the low surface tension and viscosity of THF. THF is more permeable in the surface film and easily contacts to the lithium metal surface to form large amounts of organic compounds.

The SEM graphs of lithium electrodeposited on lithium metal immersed in PC containing 1.0 M $LiBF_4$ or $LiPF_6$ for 10 min or 3 days are shown in Fig. 2. The formation of lithium dendrites is clearly observed on the lithium surface in Fig. 2(a)–(c). In the case of the deposition of lithium on a surface covered with the organic compounds formed by the direct reaction between lithium and THF electrolyte, lithium dendrites were also easily formed. On the other hand, the morphology of the electrodeposited lithium on a lithium surface immersed in PC containing 1.0 M $LiPF_6$ for 3 days is not dendritic, but hemi-spherical as shown in Fig. 2(d). From these SEM observations, we see that the morphology of lithium deposited on the lithium surface depends on the surface state of lithium. The surface film on lithium immersed in PC or γ-BL containing 1.0 M $LiPF_6$ for 3 days may consist of a dense and thin LiF layer which prevents the reaction between electrolyte and lithium, and a dense and uniform Li_2O underlayer as Li^+ ion conductor. In other cases, the lithium surface may be covered with a thick and porous layer consisting of lithium compounds. If the formation of dendrites is related to the current distribution during electrodeposition, the surface film as shown in Fig. 1(d) may have a leveling effect on the current distribution, resulting from the dense and uniform surface film.

The surface modification of lithium as shown in Fig. 1(d) is considered to be caused by the acid–base reaction of the

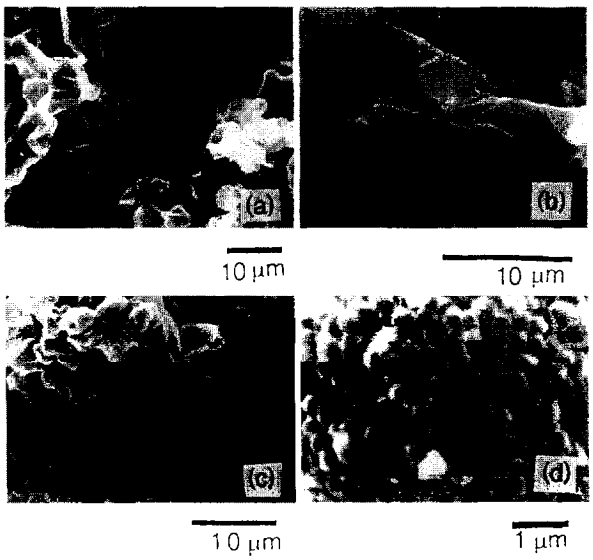

Fig. 2. SEM graphs of lithium deposited on a lithium surface immersed in: (a) 1.0 M $LiBF_4$/PC for 10 min; (b) 1.0 M $LiBF_4$/PC for 3 days; (c) 1.0 M $LiPF_6$/PC for 10 min, and (d) 1.0 M $LiPF_6$/PC for 3 days, under galvanostatic condition at 1.0 mA cm^{-2} (2 C cm^{-2}).

native film with HF added in pure PC [8,17]. A lithium metal foil was put into PC containing 5×10^{-4} M HF and 7×10^{-4} M H_2O for 3 days and the electrochemical deposition of lithium on the modified surface was performed in PC containing 1 M $LiPF_6$. Fig. 3(a) shows a SEM of lithium depos-

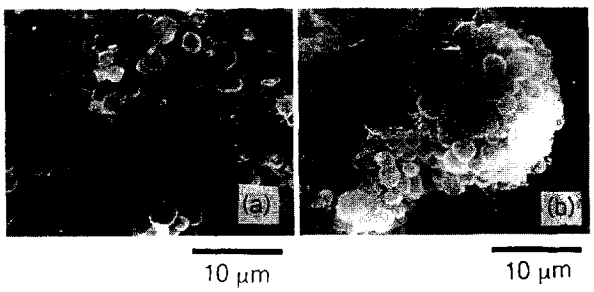

Fig. 3. SEM graphs of lithium deposited on the as-received lithium modified with the HF treatment: (a) after the first electrochemical deposition, and (b) that after five dissolution and deposition cycles, under galvanostatic condition at 0.2 mA cm^{-2} (total deposition charge: 0.48 C cm^{-2}).

ited on the modified lithium. The morphology of the deposited lithium is hemi-spherical. Even after five dissolution and deposition cycles, no dendrites are observed, as shown in Fig. 3(b). The surface film modified by HF treatment has the thin bilayer structure of LiF and Li_2O and the use of PC or γ-BL containing $LiPF_6$ enhances the suppression of the dendritic formation of lithium.

A thin and uniform surface film has a leveling effect on the current distribution for lithium electrodeposition. The lithium surface is covered with a native film. After this film was removed by argon sputtering, an ultra-thin plasma polymer layer (0.6 μm) of solid polymer electrolyte was deposited on the lithium surface in the same reactor immediately after sputtering. An ultra-thin and uniform solid polymer electrolyte layer was prepared from 1,1-difluoroethene by plasma polymerization. An SEM observation suggests that dendritic growth of lithium was suppressed on the lithium surface modified by the ultra-thin solid polymer electrolyte [18].

3. Electrodeposition and suppression of dendritic formation of lithium on a nickel substrate

On the basis of the suppression of dendritic formation of lithium on lithium foil, the electrochemical deposition of lithium on a nickel substrate was examined [9,19]. The morphology of the lithium deposited on a nickel substrate in PC containing 1.0 M $LiClO_4$ ($LiClO_4$/PC) had the typical dendrite form, and grey lithium was deposited on nickel. On the other hand, the electrodeposition of lithium was then performed in $LiClO_4$/PC containing 5×10^{-3} M HF and 7×10^{-3} M H_2O. The lithium deposited on a nickel substrate in this electrolyte had a hemispherical form, and irregular shapes were not observed. The color of the nickel electrode surface turned to brilliant blue during the electrodeposition of lithium. This indicates that the lithium surface is very smooth and uniform. A schematic illustration of the surface state of the blue lithium from XPS analysis can be drawn as shown in Fig. 4. The thickness of the surface film on deposited lithium was estimated to be about 25–50 Å, from both the XPS analysis and the impedance measurement of the surface film. Similar morphologies are also observed in

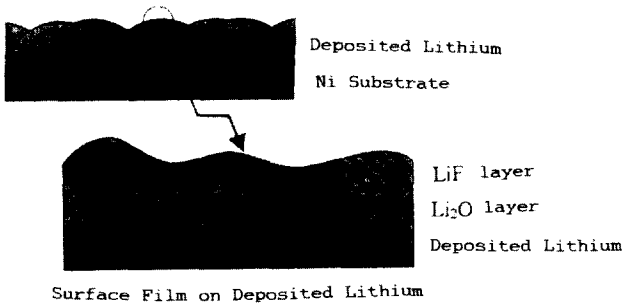

Fig. 4. Schematic illustration of the surface film of lithium deposited on a nickel substrate in 1.0 M $LiClO_4$, 5×10^{-3} M HF, and 7×10^{-3} M H_2O/PC under galvanostatic condition at 1.0 mA cm^{-2} (2 C cm^{-2}).

$LiPF_6$/PC, $LiCF_3SO_3$/PC, $LiBF_4$/PC, $LiAsF_6$/PC, $LiClO_4$/γ-BL, and $LiClO_4$/ethylene carbonate (EC) and diethyl carbonate (DEC) without HF, or containing 1×10^{-2} M HF and 1.4×10^{-2} M H_2O, as shown in Figs. 5 and 6. Thus, it can be concluded that the dense and thin bilayer of LiF and Li_2O formed on the lithium surface by the addition of small amounts of HF and H_2O to the electrolyte is very effective in suppressing the formation of lithium dendrites.

After five discharge and charge cycles in $LiClO_4$/PC containing 1.0×10^{-2} M HF and 1.4×10^{-2} M H_2O, the elec-

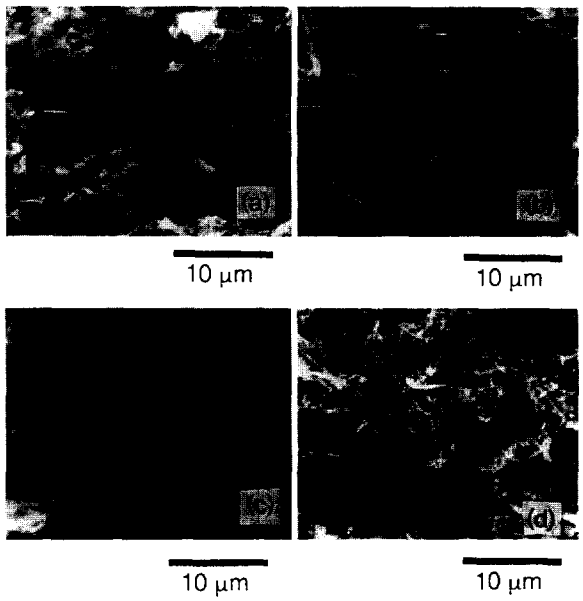

Fig. 5. SEM graphs of lithium deposited on a nickel substrate in: (a) 1.0 M $LiCF_3SO_3$/PC; (b) 1.0 M $LiBF_4$/PC; (c) 1.0 M $LiAsF_6$/PC, and (d) 1.0 M $LiClO_4$/EC+DEC, under galvanostatic condition at 1.0 mA cm^{-2} (1.0 C cm^{-2}).

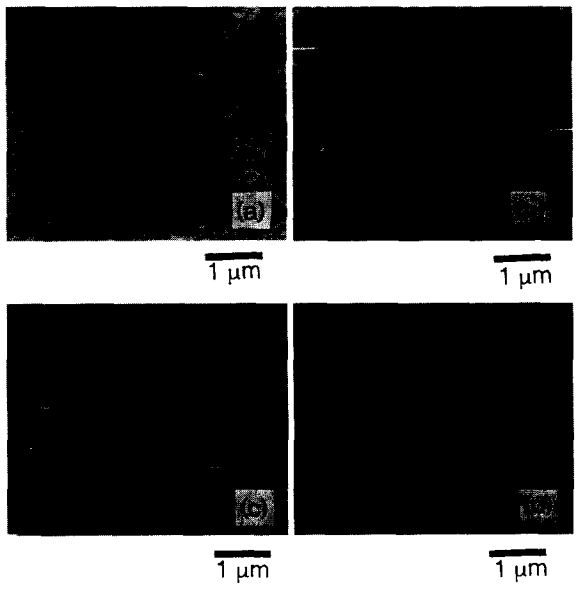

Fig. 6. SEM graphs of lithium deposited on a nickel substrate in (a) 1.0 M $LiCF_3SO_4$/PC; (b) 1.0 M $LiBF_4$/PC; (c) 1.0 M $LiAsF_6$/PC, and (d) 1.0 M $LiClO_4$/EC+DEC, containing 1.0×10^{-2} M HF and 1.4×10^{-2} M H_2O, under galvanostatic condition at 1.0 mA cm^{-2} (1.0 C cm^{-2}).

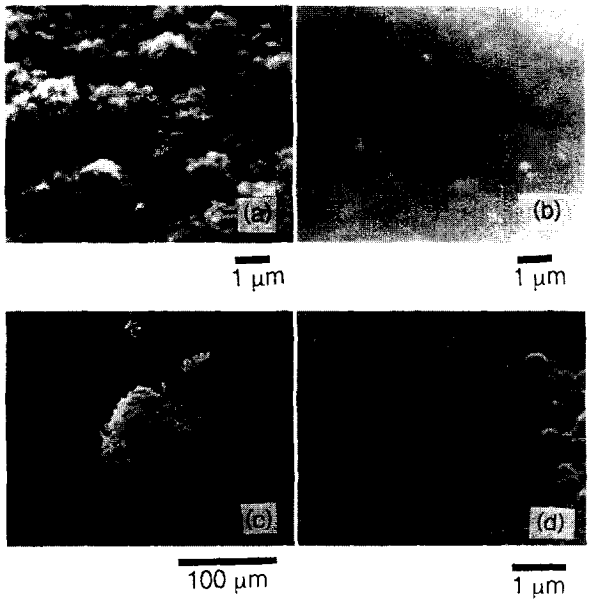

Fig. 7. SEM graphs of lithium deposited on a nickel substrate in 1.0 M $LiClO_4$/PC containing 1.0×10^{-2} M HF and 1.4×10^{-2} M H_2O after: (a) 2nd charge; (b) 5th charge; (c) 20th charge, and (d) on another nickel substrate in the electrolyte in which 20 cycles were already performed; (charge/discharge current density: 1.0 mA cm^{-2}, amount of electricity of charge: 1.0 C cm^{-2}, cut-off potential for discharge: 1.0 V vs. Li/Li^+).

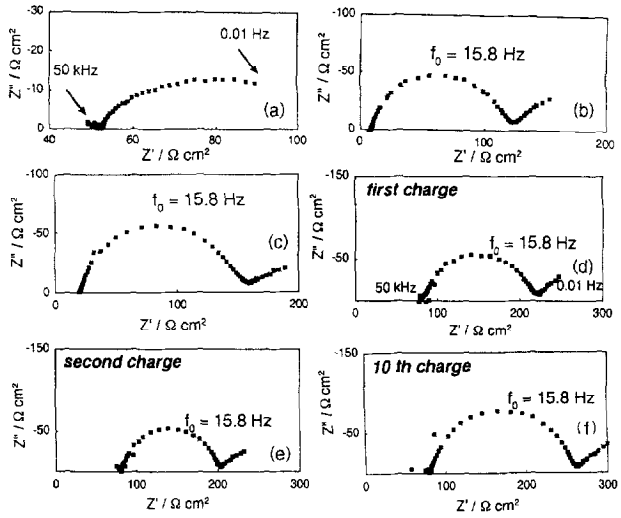

Fig. 8. Cole–Cole plots for lithium deposited on a nickel substrate in: (a) 1.0 M $LiCF_3SO_3$/PC without HF addition; (b) 1.0 M $LiClO_4$/PC; (c) 1.0 M $LiClO_4$/EC+DEC; (d) 1.0 M $LiCF_3SO_3$/PC containing 1.0×10^{-2} M HF and 1.4×10^{-2} M H_2O after 1st charge; (e) after 2nd charge, and (f) after 10th charge, under galvanostatic condition at 1.0 mA cm^{-2} (1 C cm^{-2}). Impedance measurement for lithium was performed at open-circuit voltage, the amplitude of the alternating current was 5 mV, and the frequency range was 50 kHz–0.01 Hz.

trode surface is still smooth, and no dendrite growth is observed as shown in Fig. 7(b). Thus, it can be concluded that the addition of a small amount of HF to the electrolyte is quite effective for suppressing the formation of lithium dendrites. However, after 20 discharge and charge cycles, irregularities in the lithium deposition are observed on the surface as shown in Fig. 7(c). By using the electrolyte after 20 discharge and charge cycles, lithium was deposited on another nickel substrate. The electrode surface is smooth and no dendrite growth is observed as shown in Fig. 7(d). Thus, it is concluded that the irregularities after 20 discharge and charge cycles are caused by the disturbance of uniformity of the surface film.

Cole–Cole plots for lithium deposited on a nickel substrate in various electrolytes are shown in Fig. 8. The semicircle of each Cole–Cole plot depends on the resistance of the charge transfer or that of the surface film. Since the charge-transfer resistance is considered to be about 1 Ω cm^2 from an exchange current density more than 30 mA cm^{-2} [20], the diameter of the semicircle in Fig. 8 should be due to the resistance of the surface film. A large distortion of the semicircle is observed in Cole–Cole plots for lithium deposited on a nickel substrate in the electrolyte without HF, as shown in Fig. 8(a). This may be due to the large roughness of the lithium surface, caused by the dendritic formation of lithium. On the other hand, in the case of the electrolyte containing HF, real semicircles with top-frequencies of 15.8 Hz are observed, as shown in Fig. 8(b)–(f). Thus, the surface films formed in the electrolyte containing a small amount of HF and H_2O are flat and smooth, and have almost the same structure, regardless of which electrolyte was used. On the first and second charge, almost the same surface films are observed, as shown in Fig. 8(d) and (e). But, at the 10th charge, the ionic conductivity of the surface film is somewhat decreased with the accumulation of the LiF and Li_2O layer on the lithium surface, as shown in Fig. 8(f).

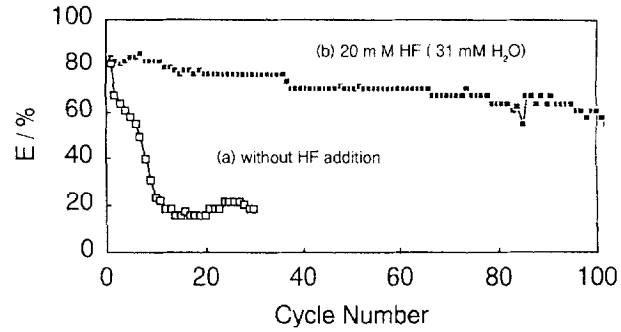

Fig. 9. Cycle efficiency changes of lithium deposited on a nickel substrate in: (a) 1.0 M $LiCF_3SO_3$/PC without HF addition, and (b) containing 2.0×10^{-2} M HF and 3.1×10^{-2} M H_2O, under galvanostatic condition at 1.0 mA cm^{-2} (1 C cm^{-2}, cut-off potential for discharge; 1.0 V vs. Li/Li^+).

Cycle efficiency changes for the lithium electrodeposited on a nickel substrate are shown in Fig. 9. Though the addition of a small amount of HF to the electrolyte is effective for the suppression of lithium dendrite formation, its effect is decreased with discharge and charge cycles. The search for a stable surface film on the deposited lithium after longer discharge and charge cycles is important for the practical use of lithium metal anodes. By such research, lithium metal anodes may be used in rechargeable batteries.

References

[1] S. Megahed and B. Scrosati, *The Electrochemical Society, Interface, 4* (4) (1995) 34–37.

[2] Z. Takehara and K. Kanamura, *Electrochim. Acta, 38* (1993) 1169–1177.

[3] D. Aurbach, A. Zaban, Y. Gofer, Y. Ein-Ely, I. Weissman, O. Chusid and O. Abramson, *J. Power Sources, 54* (1995) 76–84.

[4] D. Aurbach, Y. Ein-Eli, O. Chusid, Y. Carmeli, M. Babai and H. Yamin, *J. Electrochem. Soc., 141* (1994) 603–611.

[5] D. Aurbach, Y. Gofer, M. Ben-Zion and P. Aped, *J. Electroanal. Chem., 339* (1992) 451–471.

[6] D. Aurbach and O. Chusid, *J. Electrochem. Soc., 140* (1993) L155–157.

[7] T. Osaka, T. Momma, T. Tajima and Y. Matsumoto, *J. Electrochem. Soc., 142* (1995) 1057–1060.

[8] K. Kanamura, S. Shiraishi and Z. Takehara, *Chem. Lett.*, (1995) 209–210.

[9] K. Kanamura, S. Shiraishi and Z. Takehara, *J. Electrochem. Soc., 141* (1994) L108–110.

[10] M. Ishikawa, S. Yoshitake, M. Morita and Y. Matsuda, *J. Electrochem. Soc., 141* (1994) L159–161.

[11] T. Hirai, I. Yoshimatsu and J. Yamaki, *J. Electrochem. Soc., 141* (1994) 611–614.

[12] K. Kanamura, H. Tamura and Z. Takehara, *J. Electroanal. Chem., 333* (1992) 127–142.

[13] K. Kanamura, H. Tamura, S. Shiraishi and Z. Takehara, *Electrochim. Acta, 40* (1995) 913–921.

[14] K. Kanamura, H. Tamura, S. Shiraishi and Z. Takehara, *Denki Kagaku, 61* (1993) 1377–1382.

[15] K. Kanamura, H. Tamura, S. Shiraishi and Z. Takehara, *J. Electrochem. Soc., 142* (1995) 340–347.

[16] K. Kanamura, S. Shiraishi, H. Tamura and Z. Takehara, *J. Electrochem. Soc., 141* (1994) 2379–2385.

[17] S. Shiraishi, K. Kanamura and Z. Takehara, *J. Appl. Electrochem., 25* (1995) 584–591.

[18] Z. Takehara, Z. Ogumi, Y. Uchimoto, K. Yasuda and H. Yoshida, *J. Power Sources, 43/44* (1993) 377–383.

[19] K. Kanamura, H. Tamura, S. Shiraishi and Z. Takehara, *J. Electroanal. Chem., 394* (1995) 49–62.

[20] M.W. Verbrugge and B.J. Koch, *J. Electroanal. Chem., 367* (1994) 123–129.